IEEE Access
Multidisciplinary | Rapid Review | Open Access Journal

Received November 29, 2021, accepted December 5, 2021, date of publication December 22, 2021,
date of current version January 5, 2022.

Digital Object Identifier 10.1109/ACCESS.2021.3137388

A Robust Sensor and Actuator Fault Tolerant Control Scheme for Nonlinear System

MUHAMMAD AMMAR ASHRAF[1], SALMAN IJAZ[2], UMAIR JAVAID[3], SHARIQ HUSSAIN[4], HARIS ANWAAR[5], AND MOHAMED MAREY[6]

[1]School of Automation and Electrical Engineering, University of Science and Technology, Beijing 100083, China
[2]Key Laboratory of More Electric Aircraft Technology of Zhejiang Province, University of Nottingham, Ningbo 315104, China
[3]College of Automation Engineering, Nanjing University of Aeronautics and Astronautics, Nanjing 210016, China
[4]Department of Software Engineering, Foundation University Islamabad, Islamabad 44000, Pakistan
[5]Electrical Engineering Department, University of Engineering and Technology (UET) New Campus, Lahore 54890, Pakistan
[6]Smart Systems Engineering Laboratory, College of Engineering, Prince Sultan University, Riyadh 11586, Saudi Arabia

Corresponding author: Salman Ijaz (salman.ijaz@nottingham.edu.cn)

ABSTRACT In this article, a new fault-tolerant control (FTC) method is presented for the Lipschitz nonlinear systems that is capable of handling the actuator faults, sensor faults, unknown external disturbances, and system uncertainties. An augmented system is first constructed by treating the sensor fault as an auxiliary state. An adaptive fault estimation scheme with an H_∞ performance criterion is then developed to simultaneously estimate the actuator and sensor faults. To achieve the tracking control, a nonlinear sliding mode-based state feedback control law is proposed depending on the estimated states and information about fault from the fault estimating unit. The efficacy of the suggested technique is evaluated using a nonlinear model of the multirotor unmanned aerial vehicle (UAV) system with six degrees-of-freedom (DoF) motion. The proposed method is implemented in the inner loop subsystem in order to obtain the attitude and altitude tracking while the outer-loop control is simply a PID controller. Several simulations on the nonlinear system are performed to prove the effectiveness of the proposed method compared with the existing methods.

INDEX TERMS Actuator faults, affine nonlinear system, adaptive control, nonlinear adaptive sliding mode controller, multirotor system.

I. INTRODUCTION

Many advancements in fault detection and diagnosis, as well as fault-tolerant control (FTC), have been made in the previous decade, especially for safety-critical systems like airplanes. The FTC strategies are designed to increase the stability and security of control systems in the face of faults and failures. FTC methods for linear systems in [3] have been well developed to ensure system safety. However, a majority of systems in the real world are nonlinear, which requires an erudite FTC structure to ensure consistency of the system. Stringent control performance requirements compel the researchers to explore dominant FTC for generic nonlinear systems. The FTC strategy, in [4], developed an adaptive neural FTC approach to nonlinear structures. FTC can ensure the flying performance of UAVs if there is an actuator or sensor fault.

Sensor and actuator faults are the main cause of systems accidents. To identify the actuator and sensor faults, the fault detection and isolation (FDI) methods have been extensively adopted. For identified faults, the controller's structure can be modified to provide the system with the best reaction or halt the system operation in case of an emergency. Several FTC approaches dealing with the actuator and sensor faults have been developed. For example, a neural adaptive observer-based sensor and actuator fault recognition control for an unmanned aerial vehicle (UAV) in [5], where parameters are restructured using the extended Kalman filter. A virtual actuator and sensor FTC of the LPV system is discussed in [6] for a two-tank system. In [7], a Polynomial Fuzzy Unknown Input Observer (PFUIO) is proposed to estimate sensor and actuator faults to get the desired performance and avoid system instability. An active

The associate editor coordinating the review of this manuscript and approving it for publication was Guillermo Valencia-Palomo.

FTC technique for wind turbine systems with sensor and actuator faults is discussed in [8] using robust dynamic inversion observer and control allocation. Sliding mode control (SMC) has been employed in a range of nonlinear systems, and it is a promising option for coping with actuator failures and model uncertainties. [9], [10].

With the increase in UAV's practical applications, the main concern is maneuvering control due to complex weather conditions as UAVs fly near the earth. The UAVs FDI and FTC have gained more attention from researchers due to their critical role in the safety and reliability of the dynamic system in the last decade. A hybrid control formation for the quadrotor control is presented in [11] by combining the PID and integral sliding mode control (ISMC). The authors in [12] used an unknown input observer (UIO) design to handle the FDI ambiguity. Robust H_∞ observer design is introduced by [13], whose practical convergence is verified employing the Euler approximate discrete-time model. Quadrotor, however, cannot tolerate the complete loss of a single actuator as it lacks control redundancy. The goal of the FTC approach for multi-copters with more than four rotors is to preserve a normal and steady flying path. Additionally, provides a complete operational power even under the complete failure condition of one or more rotors. The authors in [14] created a state feedback control system based on linear-quadratic-regular (LQR) to assure stable flight. Ref. [15] proposed a full fault recognition, analysis, and system retrieval strategy for a coaxial octorotor. In [16], a coaxial octorotor helicopter controller is developed using a radial base function neural network and a fuzzy logic control technique. In [17], a PID controller is designed for UAV system elevation and vectored thrust, and then a Linear Quadratic controller is developed for UAV aircraft model predictive control. In earlier work [18], an SMC law with an adaptive gain is constructed for a multi-rotor platform that can manage actuator failures. The adaptive approach is used with the SMC law to ensure that the system is resistant to unexpected failures. An octorotor Lipschitz nonlinear model in [19] is developed, and a fault diagnostic technique for the octorotor with actuator faults was created using an ISMC.

Though a significant amount of studies have been done on FTC for UAVs with actuator issues, very few studies have dealt with sensor errors. Attempts have been made to solve the sensor error problem by transforming the sensor faults into actuator faults, such as [20], [21]. A quadrotor Lipschitz nonlinear model is characterized in [22], and a fault diagnostic technique with actuator and sensor faults was created using Thau's observer. Ref. [23] looked at a defect diagnosis challenge for UAV with numerous sensor problems. In several papers, time-varying observers are utilized in diagnosing sensor errors in UAVs. A robust fault detection approach for UAVs featuring sensor problems was presented in [24]. A Reduced-order time-varying observer was used to solve the fault diagnostic equivalence for UAVs sensor failures [25]. In reality, a little comprehensive study of the FTC issue for octorotor having sensor failures has been conducted.

Lipschitz nonlinear systems have sparked academics' interest as a special class of nonlinear systems in recent years [26]–[29]. In practice, the global or local Lipschitz characterizes a wide range of physical systems. Therefore, this study considered a general Lipschitz nonlinear system in designing an FTC law. The objective is to maintain the system stability while tolerating the effect of actuator and sensor faults. Initially, an auxiliary structure is created by treating the sensor fault as an auxiliary state. Later, an adaptive fault estimation scheme integrated with the H_∞ performance criterion is designed to estimate system faults. The key feature of the proposed fault estimation method is to detect the actuator and sensor faults simultaneously, despite the uncertainty/disturbance effect on the system dynamics. The proposed FTC law is composed of three components. The first one is the state feedback control law to stabilize the system nominally. The second component is FTC law to mitigate the fault effect. The third component is nonlinear ISMC law to recompense the consequence of uncertainty due to estimation error, model unknown dynamics, and disturbance. Finally, the theoretical findings are verified using a multirotor UAV model to show that the proposed FTC technique is successful. Compared to the existing literature [10], [15], [18], [33], [34], the main contribution and the benefits of the proposed approach are as follows

- This work proposed a method for Lipschitz nonlinear system that can tolerate the actuator and sensor faults at the same time, whereas the previous work [10], and [18], [19] can only deal with the actuators faults.
- The combination of integral SMC law and adaptive law with baseline controller provides not only the tolerance against the faults/failure but also contributes additional robustness against the unknown/unmodeled system dynamics and chattering reduction.
- In the existing work [18], the controller is designed without fault information available to the controller. However, in this work, the estimated fault (sensor and actuator) information is fed to the control input, and estimation error is coped up using nonlinear adaptive SMC law.
- The effectiveness of the proposed scheme is validated using nonlinear simulations on the 6-DOF model of multirotor UAV system with dual rotor redundancy. The comparison with the existing results [18], [34] shows that the proposed scheme is more effective in coping with both actuator and sensor faults while preserving nominal path tracking.

II. FORMULATION OF PROBLEM

Consider a Lipschitz nonlinear system that is affected by the actuator and sensor faults, described as

$$\begin{aligned} \dot{x}_p(t) &= A_p x_p(t) + B_p u_p(t) + E_p f_a(t) + f_p(x_p, t) \\ &\quad + M_p \zeta_p(t) \\ y_p(t) &= C_p x(t) + N_s f_s(t) \end{aligned} \tag{1}$$

where, $y_p(t) \in \mathbb{R}^p, u_p(t) \in \mathbb{R}^m, x_p(t) \in \mathbb{R}^n, f_s(t) \in \mathbb{R}^s$, $f_a(t) \in \mathbb{R}^r$ and $\zeta_p(t) \in \mathbb{R}^q$ represent the output vector, input vector, state vector, sensor faults, actuator faults and disturbance input vector respectively. The function $f_p(t) \in \mathbb{R}^n$, represents the Lipschitz nonlineartiy and $m \geq p$. In (1), $A_p \in \mathbb{R}^{n\times n}$, $B_p \in \mathbb{R}^{n\times m}$, $C_p \in \mathbb{R}^{p\times n}$, $M_p \in \mathbb{R}^{n\times q}$, $E_p \in \mathbb{R}^{n\times r}$ and $N_s \in \mathbb{R}^{p\times s}$ represent all the constant matrices in the system. The following assumptions are established before the rest of the analysis.

Assumption 1 [35]: The nonlinear function $f_p(x_p, t)$ is assumed to fulfill the Lipschitz condition with respect of $x_p(t)$ for all $t \geq 0$ that is $\|f_p(x_{p_1}, t) - f_p(x_{p_2}, t)\| \leq \gamma_p \|x_{p_1} - x_{p_2}\|$, where γ_p is the known positive Lipschitz constant.

Assumption 2 [36]: The pair (A_p, B_p) is controllable and (A_p, C_p) is detectable.

Assumption 3 [37]: The actuator fault, sensor fault, and disturbance are all considered to be confined in the following way

$$\begin{aligned} &\|\zeta_p(t)\| < \bar{\zeta}_p, \quad \|f_s(t)\| \leq \bar{f}_s, \ \|\dot{f}_s(t)\| \leq \bar{f}_{s_1} \\ &\|f_a(t)\| \leq \bar{f}_a, \text{ and } \|\dot{f}_a(t)\| \leq \bar{f}_{a_1} \end{aligned} \tag{2}$$

Lemma 1 [30]: The following inequality holds for a scalar μ and a positive definite matrix $P > 0$

$$2x^T y \leq \frac{1}{\mu} x^T P x + \mu y^T P^{-1} y \quad x, y \in \mathbb{R}^n \tag{3}$$

A filtered version of sensor faulty signal $y_p(t)$ is defined as

$$\begin{aligned} \dot{\omega}_p(t) &= -A_f \omega_p(t) + A_f y_p(t) \\ &= -A_f \omega_p(t) + A_f C_p x_p(t) + A_f N_s f_s(t) \end{aligned} \tag{4}$$

where, $A_f \in \mathbb{R}^{p\times p}$ is a stable filter matrix and $\omega_p(t) \in \mathbb{R}^p$. Next define an augmented system of order $n + p$ that is obtained by combining Lipschitz nonlinear system (1) and filtered version (4) as

$$\begin{aligned} \underbrace{\begin{bmatrix} \dot{x}_p(t) \\ \dot{\omega}_p(t) \end{bmatrix}}_{x(t)} &= \underbrace{\begin{bmatrix} A_p & 0 \\ A_f C_p & -A_f \end{bmatrix}}_{A} \underbrace{\begin{bmatrix} x_p(t) \\ \omega_p(t) \end{bmatrix}}_{x(t)} + \underbrace{\begin{bmatrix} B_p \\ 0 \end{bmatrix}}_{B} u_p(t) \\ &+ \underbrace{\begin{bmatrix} E_p & 0 \\ 0 & A_f N_s \end{bmatrix}}_{E} \underbrace{\begin{bmatrix} f_a(t) \\ f_s(t) \end{bmatrix}}_{f_f(t)} + \underbrace{\begin{bmatrix} f_p(x,t) \\ 0 \end{bmatrix}}_{f(x,t)} + \underbrace{\begin{bmatrix} M_p \\ 0 \end{bmatrix}}_{M} \zeta_p(t) \end{aligned} \tag{5}$$

The augmented system (5) can generally be written as

$$\begin{aligned} \dot{x}(t) &= Ax(t) + Bu_p(t) + Ef_f(t) + f(x,t) + M\zeta_p(t) \\ y(t) &= Cx(t) \end{aligned} \tag{6}$$

where $f(x, t) \in \mathbb{R}^{n+p}$ represent the Lipschitz nonlinear function of augmented system, $x(t) \in \mathbb{R}^{n+p}$ is a new state vector, $y(t) \in \mathbb{R}^{p+p}$ denotes the new output vector, $f_f(t) \in \mathbb{R}^{r+s}$ shows the sensor and actuator fault, $A \in \mathbb{R}^{(n+p)\times(n+p)}$, $B \in \mathbb{R}^{(n+p)\times m}$, $C \in \mathbb{R}^{(p+p)\times(n+p)}$, $E \in \mathbb{R}^{(n+p)\times(r+s)}$ and $M \in \mathbb{R}^{(n+p)\times q}$ shows the matrices of augmented system.

Assumption 4 [37]: The augmented fault signal $f_f(t)$ and the rate are also assumed to be bounded, i.e. $\|f_f(t)\| \leq \bar{f}_f$ and $\dot{f}_f(t) \leq \bar{f}_{f_1}$.

III. FAULT TOLERANT CONTROLLER DESIGN

This section developed FTC strategy for the Lipschitz nonlinear system (1) that can compensate for the actuator fault and sensor fault while maintaining the system response to the desired path. First, an adaptive observer is created to estimate sensor failures, and actuator faults. Then, an ISMC law is developed that utilizes fault data to reconfigure nominal law such that the closed-loop system stability is ensured. The control architecture of the proposed FTC law is provided in Figure 1.

A. ADAPTIVE OBSERVER-BASED FAULT ESTIMATION SCHEME

For the augmented nonlinear system (5), the structure of adaptive observer is defined as

$$\begin{aligned} \dot{\hat{x}}(t) &= A\hat{x}(t) + Bu_p(t) + f(\hat{x}, t) + G_L e_y(t) + E\hat{f}_f(t) \\ \dot{\hat{y}}(t) &= C\hat{x}(t) \end{aligned} \tag{7}$$

where $\hat{x}(t)$ and $\hat{y}(t)$ represent the estimated state and output vectors, $f(\hat{x}, t)$ denotes the Lipschitz nonlinear function with respect to estimated states $\hat{x}(t)$, $G_L \in \mathbb{R}^{(n\times p)\times(p+p)}$ is the observer gain, $e(t) = x(t) - \hat{x}(t)$ defines the state estimation error and $\hat{f}_f(t)$ constitutes of estimation of fault. Next, taking error function $e(t)$ time derivative and substitute (1) and (7) which yields

$$\begin{aligned} \dot{e}(t) = (A - G_L C)e(t) + Ee_f(t) + f(x,t) - f(\hat{x},t) \\ + M\zeta_p(t) \end{aligned} \tag{8}$$

where $e_f(t) = f_f(t) - \hat{f}_f(t)$.

Theorem 1: Under the assumptions 1-4, if we apply the state observer (7) to the system (6) and there exists a constant $\epsilon_p > 0$, and symmetric positive definite matrix $P_1 = P_1^T > 0$, the matrices $Y_1 \in \mathbb{R}$ and $G_1 > 0$ such that the following conditions hold

$$\begin{bmatrix} A_{cl} & * & P_1 M & P_1 \\ * & G_1 + I & * & * \\ * & * & -\bar{\epsilon}_p I & * \\ * & * & * & -\bar{\gamma}_p I \end{bmatrix} < 0 \tag{9}$$

$$E^T P_1 = R_1 C \tag{10}$$

where $A_{cl} = A^T P_1 - C^T Y^T + P_1 A - Y_1 C + C^T C + I_p$, $R_1 \in \mathbb{R}^{(r+s)\times(p+p)}$, $\bar{\epsilon}_p = \epsilon_p^2$, $\bar{\gamma}_p = \gamma_p^2$, and $\eta_p = \bar{f}_{f_1}^2 \lambda_{max}(\Gamma^{-1} G_1^{-1} \Gamma^{-1})$, then the fault estimation algorithm $\hat{f}_f(t)$

$$\dot{\hat{f}}_f(t) = \Gamma R_1 e_y(t) \tag{11}$$

can guarantee $e(t)$ and $e_f(t)$ as uniformly ultimately bounded, where $e_y(t) = C(x(t) - \hat{x}(t))$ and $\Gamma \in \mathbb{R}^{(r+s)\times(r+s)}$ is symmetric positive definite matrix defined as learning rate.

Proof: Consider the Lyapunov function

$$V(t) = e^T(t) P_1 e(t) + e_f^T(t) \Gamma^{-1} e_f(t) \tag{12}$$

The time derivative of Lyapunov function (12) after substituting the dynamics of error system (8) gives

$$\dot{V}_1(t) = \dot{e}^T(t) P_1 e(t) + e^T P_1 \dot{e}(t) + 2e_f^T(t) \Gamma^{-1} \dot{e}_f(t)$$

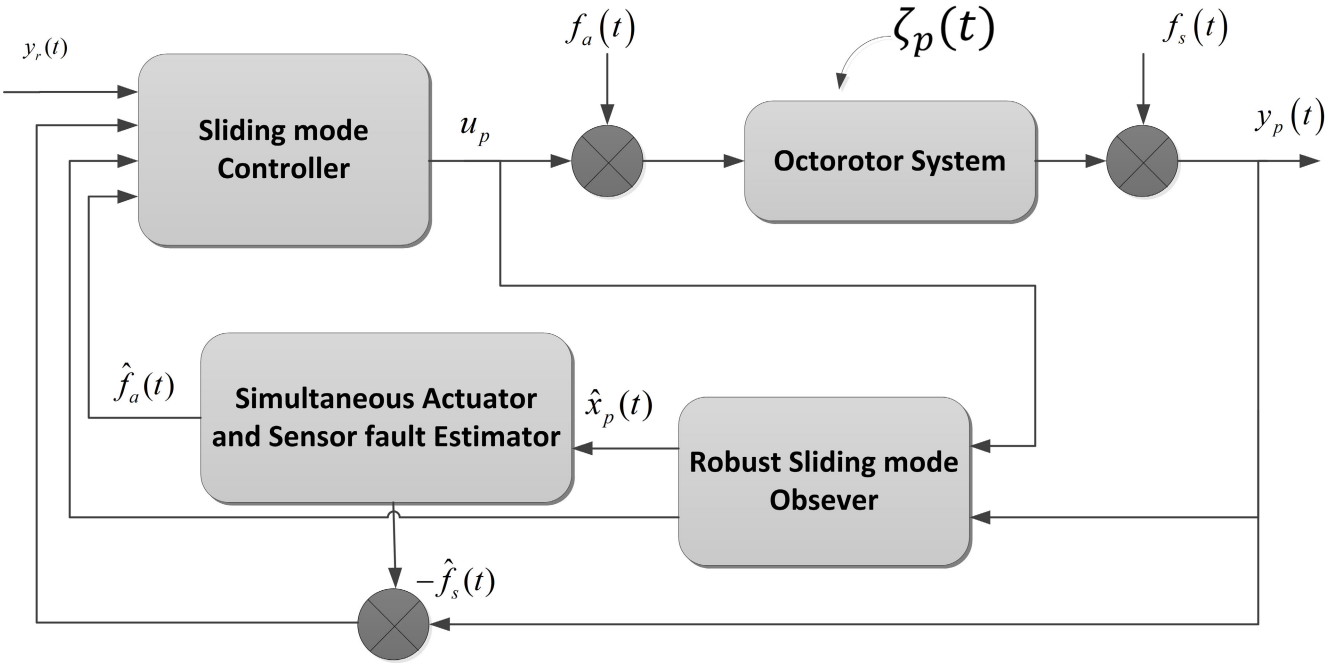

FIGURE 1. Architecture of FTC strategy.

$$
\begin{aligned}
&= e^T(t)[(A-G_LC)^TP_1 + P_1(A-G_LC)]e(t) \\
&\quad +2e^T(t)P_1Ee_f(t) + 2e^T(t)(f(x,t)-f(\hat{x},t)) \\
&\quad +2e^T(t)P_1M\zeta_p(t) + 2e^T(t)\Gamma^{-1}\dot{e}_f(t) \qquad (13)
\end{aligned}
$$

Next, substituting the adaptive law (11) into (13), we get

$$
\begin{aligned}
\dot{V}_1(t) &= e^T(t)[(A-G_LC)^TP_1 + P_1(A-G_LC)]e(t) \\
&\quad +2e^T(t)P_1Ee_f(t) + 2e^T(t)P_1(f(x,t)-f(\hat{x},t)) \\
&\quad +2e^T(t)P_1M\zeta_p(t) + 2e_f^T(t)\Gamma^{-1}\dot{f}_f(t) \\
&\quad -2e_f^T(t)\Gamma^{-1}\Gamma R_1e_y(t) \qquad (14)
\end{aligned}
$$

It follows from Eq(10)

$$
2e^TP_1Ee_f(t) - 2e_f^T(t)R_1Ce(t) = 0 \qquad (15)
$$

Using the assumption 1, we have

$$
2e^T(t)P_1(f(x,t)-f(\hat{x},t)) \le \gamma_p^2e^T(t)P_1^TP_1e(t) + e^T(t)e(t) \qquad (16)
$$

Based on the Lemma 1 and assumption 4, it can be deduced as

$$
\begin{aligned}
2e_f^T(t)\Gamma^{-1}\dot{f}_f(t) &\le e_f^T(t)G_1e_f(t) + \dot{f}_f^T(t)(\Gamma^{-1}G_1^{-1}\Gamma^{-1})\dot{f}(t) \\
&\le e_f^T(t)G_1e_f(t) + \underbrace{\bar{f}_{f_1}^2\lambda_{max}(\Gamma^{-1}G_1^{-1}\Gamma^{-1})}_{\eta_e} \qquad (17)
\end{aligned}
$$

Next substituting (15-17) into (14), we get

$$
\begin{aligned}
\dot{V}_1(t) &\le e^T(t)[(A-G_LC)^TP_1 + P_1(A-G_LC)]e(t) \\
&\quad +\gamma_p^2e^T(t)P_1^TP_1e(t) + e^T(t)e(t) + 2e^TP_1M\zeta_p(t) \\
&\quad +e_f^T(t)G_1e_f(t) + \eta_e + e_f^T(t)e_f(t) \qquad (18)
\end{aligned}
$$

To induce the robustness against the external disturbance, the H_∞ tracking index is selected as

$$
J = \int_0^\infty e_y^T(t)e_y(t) - \varepsilon_1^2\zeta_p^T(t)\zeta_p(t)dt \qquad (19)
$$

for initial condition $V(0) = 0$, $V(\infty) > 0$, we obtain

$$
\begin{aligned}
J &= \int_0^\infty [e_y^T(t)e_y(t) - \varepsilon_1^2\zeta_p^T(t)\zeta_p(t) \\
&\quad +\dot{V}_1(t)]dt + V(0) - V(\infty) \\
&\le \int_0^\infty e^T(t)C^TCe(t) - \varepsilon_1^2\zeta_p^T(t)\zeta_p(t) + \dot{V}_1(t)dt \qquad (20)
\end{aligned}
$$

The term inside the integral in (20) is defined as

$$
\begin{aligned}
\mathcal{N} &= e^T(t)C^TCe(t) - \varepsilon_1^2\zeta_p^T(t)\zeta_p(t) + e^T(t)[(A-G_LC)P_1 \\
&\quad +P_1(A-G_LC) + \gamma_p^2P_1^TP_1 + I] + e_f^T(t)G_1e_f(t) \\
&\quad +2e^T(t)P_1M\zeta_p(t) + \eta_e + e_f(t)e_f(t) \\
&= \underbrace{\begin{bmatrix} e(t) \\ e_f(t) \\ \zeta_p(t) \end{bmatrix}^T}_{\gamma_f^T(t)} \underbrace{\begin{bmatrix} A_{cl} & 0 & P_1M \\ 0 & G_1+I & 0 \\ 0 & 0 & -\epsilon_1^2I \end{bmatrix}}_{\Xi} \underbrace{\begin{bmatrix} e(t) \\ e_f(t) \\ \zeta_p(t) \end{bmatrix}}_{\gamma_f(t)} + \eta_e \qquad (21)
\end{aligned}
$$

where $A_{cl} = (A-G_LC)^TP_1 + P_1(A-G_LC) + \gamma_p^2P_1P_1 + C^TC + I$. Finally (21) is obtained as

$$
\mathcal{N} = \gamma_f^T(t)\Xi\gamma_f(t) + \eta_e \qquad (22)
$$

When $\Xi < 0$ we can obtain $\dot{V}_1(t) < -\varepsilon_o\|\gamma_f\|^2 + \eta_e$, where $\varepsilon_o = \lambda_{max}(-\Xi)$. As a consequence, $\dot{V}_1(t) < 0$ for $\varepsilon_o\|\gamma_f\|^2 > \eta_e$ that is to say $(e(t), e_f(t))$ coheres to a finite set accordingly to Lyapunov stability theorem. As a result, the fault and state estimation errors $(e(t), e_f(t))$ are uniformly bounded.

This ends the proof. Next it is not possible to solve (9) and (10) simultaneously, therefore eq(10) is transformed into LMI defined as [38].

Minimize η subject to the following

$$\begin{vmatrix} \eta I & E^T P_1 - R_1 C \\ (E^T P_1 - R_1 C)^T & \eta I \end{vmatrix} > 0 \tag{23}$$

B. DEVELOPMENT OF FTC LAW

The estimated states and fault information from the fault estimation unit, proposed in the last subsection, are utilized to design FTC law for nonlinear system (1). The control law for the nonlinear system (1) is defined as

$$u_p(t) = u_{p_l}(t) + u_{p_c}(t) + u_{p_n}(t) \tag{24}$$

where $u_{p_l}(t) = -F_p x_p(t)$ is the linear control law and $F_p \in \mathbb{R}^{m\times n}$ denotes the gain in feedback path. The gain is selected by adopting the LMI synthesis procedure in order to make the dynamics of CLS

$$\dot{x}_p(t) = (A_p - B_p F_p)x_p(t) + f_p(x,t) \tag{25}$$

stable, where $u_{p_c}(t) = -E_p\hat{f}_a(t)$ is the fault compensator term and $u_{p_n}(t)$ is the nonlinear ISMC law that provide the robustness to the closed-loop system.

Proposition 1: For the nominal system (no external disturbance $\zeta_p(t) = 0$) with the feedback control law $u_{p_l}(t)$. The origin is exponential stable if there exist a constant $\lambda > 0$, a matrix $W_2 \in \mathbb{R}^{m\times n}$, and a symmetric positive definite matrix $Q_2 \in \mathbb{R}^{n\times n}$ such that

$$\begin{bmatrix} A_p Q_2 + Q_2 A_p - W_2^T B_p^T & & \\ -BW_2 + \frac{1}{\lambda_p} I_n & Q_2 & \\ Q_2 & & -\frac{1}{\gamma_p \lambda_p} I_n \end{bmatrix} < 0 \tag{26}$$

where the feedback gain F_p is obtained from $F_p = W_2 Q_2^{-1}$.

Proof: Choosing a Lyapunov function defined as

$$V_p(t) = x_p^T(t) P_2 x_p(t) \tag{27}$$

where $P_2 \in \mathbb{R}^{n\times n}$ is positive definite matrices. The derivative of Lyapunov function (27) after substituting (25) is written as

$$\dot{V}_p(t) = x_p^T\left[(A_p - B_p F_p)^T P_2 + P(A_p - B_p F_p)\right]x_p(t) + 2f_p(x_p,t)P_2 x_p(t) \tag{28}$$

Finally using the Lemma 1, the above equation can be written as

$$\dot{V}_p(t) \le x_p^T(t)\left[(A_p - B_p F_p)^T P_2 + P_2(A_p - B_p F_p)\right]x_p(t) + \gamma_p^2 \lambda_p I_n + \frac{1}{\lambda_p} P_2^T P_2 \tag{29}$$

The negative definiteness of Lyapunov function $\dot{V}_p(t)$ implies

$$(A_p - B_p F_p)^T P_2 + P_2(A_p - B_p F_p) + \gamma_p^2 \lambda_p P_2^T P_2 + \lambda_p^{-1} I_n < 0 \tag{30}$$

If we substitute $Q_p = P_2^{-1}$, $W_2 = F_p Q_2$ and apply the Schur complement, the inequality (30) is equivalent to (26). This complete the proof.

In the control law (24), the term $u_{p_n}(t)$ is designed using ISMC technique and is as follows

$$u_n(t) = -\rho(t,\hat{x}_p)\frac{\delta_p(t)}{\|\delta_p(t)\|} \tag{31}$$

where the switching function $\delta_p(t)$ is defined as

$$\delta_p(t) = G_p\hat{x}_p(t) - G_p x_p(0) - G_p\int_0^t \big(A_p\hat{x}_p(\tau) + B_p u_{p_l}(\tau) + f(\hat{x},t) + M_p\zeta_p(t)\big)dt \tag{32}$$

where $G_p \in \mathbb{R}^{m\times n}$ is the design freedom matrix selected as

$$G_p = (B_p^T B_p)^{-1} B_p^T \tag{33}$$

In (31), $\rho(t,\hat{x}_p(t))$ varies according to the following adaptive law

$$\begin{aligned} \rho(t,\hat{x}_p) &= \|F_p\|\|\hat{x}_p(t)\|\bar{\rho}(t,\hat{x}_p) + \eta_s \\ \dot{\bar{\rho}}(t,\hat{x}_p) &= \|F_p\|\|\hat{x}_p(t)\|\|\delta_p(t)\| \end{aligned} \tag{34}$$

where $\bar{\rho}(t,\hat{x}_p(t))$ denotes the positive adaption gain, η_s is the positive define scalar and $\hat{x}_p(t)$ denotes the estimated state error for system (1) defined as

$$\dot{\hat{x}}_p(t) = A_p\hat{x}_p(t) + E_p\tilde{f}_a(t) + f_p(\hat{x}_p,t) + G_{L_p}e_{y_p}(t) \tag{35}$$

where $G_{L_p} \in \mathbb{R}^{n\times p}$, and $e_{y_p}(t) = C_p(x_p(t) - \hat{x}_p(t))$.

Proposition 2: The control law (24) along with the sliding mode component defined in (31) will maintain the sliding onto the sliding surface $\{\mathcal{S}_p = \hat{x}_p(t) \in \mathbb{R}^n : \delta_p(t) = 0\}$, if the adaption gain $\rho(t,\hat{x}_p(t))$ is selected according to (34) and maximum gain ρ^* is chosen as (see appendix A)

$$\rho^* \ge \frac{\|G_p E_p\hat{f}_a(t)\| + \|G_{L_p}e_{y_p}(t)\| - \|E_p\hat{f}_a(t)\| - \|G_p M_p\zeta_p(t)\|}{\|F_p\|\|\hat{x}_p(t)\|} \tag{36}$$

Proof: First, we calculate the switching function (32) derivatives as

$$\dot{\delta}_p(t) = G_p\dot{\hat{x}}_p(t) - G_p A_p\hat{x}_p(t) - G_p B_p u_{p_l}(t) - G_p M_p\zeta_p(t) \tag{37}$$

Next, substituting $\dot{\hat{x}}_p(t)$ from (35), we will get,

$$\dot{\delta}_p(t) = G_p B_p u_p(t) + G_p E_p\hat{f}_a(t) + G_p G_{l_p}e_{y_p}(t) + G_p B_p F_p u_{p_l}(t) - G_p M_p\zeta_p(t) \tag{38}$$

Using G_p defined in (33), we can evaluate $G_p B_p = I$. Insert the design freedom matrix gain defined in (33) and the control law given in (24) into (38) we get,

$$\begin{aligned} &\dot{\delta}_p(t) \\ &= u_c(t) + u_n(t) + G_p E_p\hat{f}_a(t) + G_p G_{l_p}e_{y_p}(t) - G_p M_p\zeta_p(t) \\ &= -E_p\hat{f}_a(t) - \rho(t,\hat{x}_p)\frac{\delta_p(t)}{\|\delta_p(t)\|} + G_p E_p\hat{f}_a(t) + G_p G_{l_p}e_{y_p}(t) \\ &\quad - G_p M_p\zeta_p(t) \end{aligned} \tag{39}$$

Defining a Lyapunov function as

$$V_2(t) = \frac{1}{2}\delta_p^T(t)\delta_p(t) + \frac{1}{2}\rho_e(t,\hat{x}_p)^2 \tag{40}$$

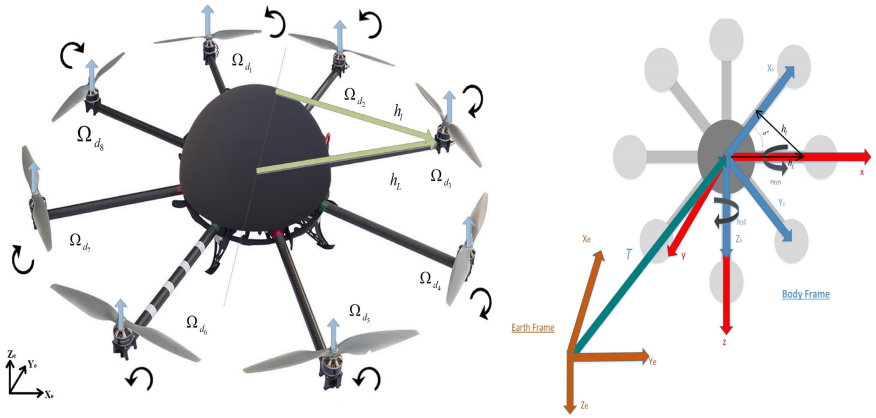

FIGURE 2. Octorotor configuration.

where $\rho_e(t,\hat{x}_p) = \bar{\rho}(t,\hat{x}_p) - \rho^*$ denotes the adaptive gain error and ρ^* denotes the bound on the modulation gain. Next substituting switching function derivative (39) and adaptive law (34) into the derivative of Lyapunov function (40), we get

$$\begin{aligned}
&\dot{V}_2(t)\\
&= \delta_p^T(t)\dot{\delta}_p(t) + \rho_e(t,\hat{x}_p)\dot{\rho}_e(t,\hat{x}_p)\\
&= \delta_p^T(t)\big(G_pE_p\hat{f}_a(t) - E_p\hat{f}_a(t) - \rho(t,\hat{x}_p)\frac{\delta_p(t)}{\|\delta_p(t)\|} + G_pG_{l_p}\\
&\quad \times e_{y_p}(t) - G_pM_p\zeta_p(t)\big) + (\bar{\rho}(t,\hat{x}_p) - \rho^*)\|F_p\|\|\hat{x}_p(t)\|\|\delta_p(t)\\
&\leq \|\delta_p^T(t)\|\big(\|G_pE_p\hat{f}_a(t)\| - \|E_p\hat{f}_a(t)\| - \rho^*\|\mathcal{F}_p\|\|\hat{x}_p(t)\|\\
&\quad -\eta_s + \|G_pG_{l_p}e_{y_p}(t)\| - \|G_pM_p\zeta_p(t)\|\big) \qquad (41)
\end{aligned}$$

Next if we choose the bound on the modulation gain (36), the Lyapunov function (41) is finally obtained as

$$\dot{V}_2 \leq -\eta_s\|\delta_p(t)\|^2 \qquad (42)$$

The proof is valid since it is equal to the η_s reachability criteria.

Remark: The discontinuity in SMC law in (31) may cause chattering in practical implementations. To avoid such situation, we utilized the sigmoidal approximation of the discontinuous function that replaced the unit vector term in (31) by

$$sign(\delta_p(t)) = \frac{\delta_p(t)}{\|\delta_p(t)\| + \rho_p} \qquad (43)$$

where ρ_p is chosen to be small scalar.

IV. APPLICATION TO MULTIROTOR UAV SYSTEM

The efficiency of the projected method is authenticated on the nonlinear model of the multirotor system. As depicted in Fig. 2, a star-shaped multirotor serves as a test platform to endorse the presented theoretical results in the previous section. Eight rotors formation is spaced equally at 45°. Some suitable assumptions for creating the multirotor model are adopted from [31] for ensuing control design. The drag and thrust coefficients are constants while hub forces and rolling moments are assumed negligible. The multirotor, like the inertia matrix, is symmetric. The nonlinear model of a multirotor system is presented in [14] as,

$$\begin{aligned}
\begin{bmatrix}\ddot{\mathcal{X}}_x\\ \ddot{\mathcal{X}}_y\\ \ddot{\mathcal{X}}_z\end{bmatrix} &= \begin{bmatrix} b_x\frac{1}{m}\tau_z\\ b_y\frac{1}{m}\tau_z\\ b_z\frac{1}{m}\tau_z - g\end{bmatrix}\\
\begin{bmatrix}\ddot{\mathcal{X}}_\phi\\ \ddot{\mathcal{X}}_\theta\\ \ddot{\mathcal{X}}_\psi\end{bmatrix} &= \begin{bmatrix} c_1\mathcal{X}_q\mathcal{X}_r - c_2\mathcal{X}_q\Omega_d + c_3\tau_\phi\\ c_4\mathcal{X}_p\mathcal{X}_r - c_5\mathcal{X}_p\Omega_d + c_6\tau_\theta\\ c_7\mathcal{X}_p\mathcal{X}_q + c_8\tau_\psi\end{bmatrix} \qquad (44)
\end{aligned}$$

where the terms

$$\begin{aligned}
b_x &= S_\phi S_\psi + C_\phi S_\theta C_\psi,\\
b_y &= -S_\phi C_\psi + S_\psi S_\theta C_\phi\\
b_z &= C_\theta C_\phi
\end{aligned}$$

and

$$c_1 = \frac{I_{yy}-I_{zz}}{I_{xx}},\quad c_2 = \frac{J_r}{I_{xx}},\quad c_3 = \frac{1}{I_{xx}},\quad c_4 = \frac{I_{zz}-I_{xx}}{I_{yy}},$$
$$c_5 = \frac{J_r}{I_{yy}},\quad c_6 = \frac{1}{I_{yy}},\quad c_7 = \frac{I_{xx}-I_{yy}}{I_{zz}},\quad c_8 = \frac{1}{I_{zz}}$$

The parameter descriptions are provided in Table 1. The model parameters are listed in Table 2. Furthermore, the residual propeller speed of unbalanced rotors is represented as [32].

$$\Omega_d = -\Omega_{d_1} - \Omega_{d_2} - \Omega_{d_5} - \Omega_{d_6} + \Omega_{d_3} + \Omega_{d_4} + \Omega_{d_7} + \Omega_{d_8} \qquad (45)$$

The nonlinear model (44) may be expressed in the following affine nonlinear form:

$$\dot{x}_p(t) = f(x_p) + g(x_p)U_\tau(t) \qquad (46)$$

where

$$x_p = [\,\mathcal{X}_x\ \mathcal{X}_y\ \mathcal{X}_z\ \mathcal{X}_\phi\ \mathcal{X}_\theta\ \mathcal{X}_\psi\ \dot{\mathcal{X}}_x\ \dot{\mathcal{X}}_y\ \dot{\mathcal{X}}_z\ \mathcal{X}_p\ \mathcal{X}_q\ \mathcal{X}_r\,]^T \qquad (47)$$

and

$$U_\tau = \begin{bmatrix}\tau_z\\ \tau_\phi\\ \tau_\theta\\ \tau_\psi\end{bmatrix} = \begin{bmatrix}\text{Total thrust}\\ \text{Roll torque}\\ \text{Pitch torque}\\ \text{Yaw torque}\end{bmatrix} \qquad (48)$$

TABLE 1. Definition of multirotor UAV system parameters.

Parameters	Definition
$\mathcal{X}_x, \mathcal{X}_y$ and $\mathcal{X}_z$	x - y translational and altitude states
$\mathcal{X}_\phi, \mathcal{X}_p$	Roll angle and angular rate
$\mathcal{X}_\theta, \mathcal{X}_q$	Pitch angle and angular rate
$\mathcal{X}_\psi, \mathcal{X}_r$	Yaw angle and angular rate
g, Ω_d	Gravitational constant, Body angular velocity
m, U_τ	Vehicle mass, Torque
I_{zz}, I_{yy}, and I_{xx}	Inertia's on z, y and x axes
I_r and I_b,	Body and rotor inertia
h_L and h_l	Arm and moment arm

TABLE 2. Parameter values.

Parameters	Symbols	Value	Unit
Gravity	g	9.81	m/s^2
Mass	m	1.64	Kg
Inertia on x-axis	I_{xx}	0.044	$Kg.m^2$
Inertia on y-axis	I_{yy}	0.044	$Kg.m^2$
Inertia on z-axis	I_{zz}	0.088	$Kg.m^2$
Drag coefficient	d	$0.3 * 10^{-6}$	$Nm.s^2$
Arm Length	h_L	0.4	m
Rotor Inertia	I_b	$90 * 10^{-6}$	$Kg.m^2$

Furthermore, the torque input U_τ is generated by varying the individual rotor speeds and is specifically defined by the following relationship

$$U_\tau = B_\Omega u_{\Omega_d} \tag{49}$$

where $u_{\Omega_d} = [\Omega_{d_1}^2, \Omega_{d_2}^2, \cdots, \Omega_{d_8}^2]^T$ and

$$B_\Omega = \begin{bmatrix} b_o & b_o & b_o & b_o & b_o & b_o & b_o & b_o \\ 0 & 0 & -b_o h_l & -b_o h_l & 0 & 0 & b_o h_l & b_o h_l \\ b_o h_l & b_o h_l & 0 & 0 & -b_o h_l & -b_o h_l & 0 & 0 \\ -h_d & -h_d & h_d & h_d & -h_d & -h_d & h_d & h_d \end{bmatrix}$$

where b_o and h_d are the thrust and drag coefficients and h_l represents the distance between the center of mass and rotor of multirotor UAV system. The multirotor nonlinear model parameters specified in (44) are derived from [33]. The dynamics of the multirotor UAV system are partitioned into two control loops in order to govern both the translational and attitude states [19]. Firstly, the inner loop, which is linked with the quicker system dynamics of altitude and rotating motion states, i.e.,

$$x_p = \left[\mathcal{X}_z \ \mathcal{X}_\phi \ \mathcal{X}_\theta \ \mathcal{X}_\psi \ \dot{\mathcal{X}}_z \ \mathcal{X}_p \ \mathcal{X}_q \ \mathcal{X}_r\right]^T \tag{50}$$

The second is the outer loop, i.e.

$$x_{out} = \left[\mathcal{X}_x \ \mathcal{X}_y \ \dot{\mathcal{X}}_x \ \dot{\mathcal{X}}_y\right]^T \tag{51}$$

The inner-loop structure is over-actuated, which can be seen in the nonlinear model (44).

V. SETTLING OF CONTROLLER PARAMETERS AND NONLINEAR SIMULATIONS

A. SETTLING OF CONTROLLER PARAMETERS

The efficacy of the proposed fault estimation and fault-tolerant control structure is verified via nonlinear simulations on octorotor UAV system. Based on the previous research [19], the nonlinear model of multirotor UAV can be expressed in Lipschitz nonlinear form defined as

$$\begin{aligned} \dot{x}_p(t) &= A_p x_p(t) + B_p u_p(t) + E_p f_a(t) + f_p(x_p, t) + M_p \zeta_p(t) \\ y(t) &= C_p x(t) + N_s f_s(t) \end{aligned} \tag{52}$$

where

$$A_p = \begin{bmatrix} 0 & I_4 \\ 0 & 0 \end{bmatrix}, \quad B_p = \begin{bmatrix} 0_{4\times4} \\ B_\tau \end{bmatrix} B_\Omega, \ C_p = I_8$$

$$B_\tau = \begin{bmatrix} 1 & 0 & 0 & 0 \\ 0 & 1/I_{xx} & 0 & 0 \\ 0 & 0 & 1/I_{yy} & 0 \\ 0 & 0 & 0 & 1/I_{zz} \end{bmatrix}, \quad E_p = \begin{bmatrix} 0_{4\times4} \\ B_\tau \end{bmatrix}$$

$$f_p(x_p, u_p, t) = \begin{bmatrix} 0_{4\times4} \\ \frac{1}{m}(b_z - 1)\tau_z \\ c_1 qr \\ c_4 pr \\ c_7 pq \end{bmatrix}, \quad N_s = \begin{bmatrix} 0_{4\times4} \\ I_4 \end{bmatrix}$$

$$M_p = \begin{bmatrix} 0_{4\times1} \ c_2 q \ c_5 r \ 0 \end{bmatrix}^T,$$

$$u_p(t) = col(u_z, \tau_\phi, \tau_\theta, \tau_\psi),$$

$$u_z = \tau_z/m - g$$

and $\zeta_p(t) = \Omega_d$. The LMI's given in (9), (23), and (26) are solved using the CVX toolbox in MATLAB and the controller and observer gains are computed as (53) and (54), shown at the bottom of the next page.

The actuator fault signal is considered as $f_a(t) = w_{p_i}(t)u_i(t)$ where $w_{p_i}(t)$ is the magnitude of the actuator fault with range $0 < w_{p_i}(t) < 1, i = 1, .., 4$, and $u_{p_i}(t)$ denotes the torque input to the system. In this paper, two types of sensor faults are taken into account; one is bias fault and other is sinewave sensor fault. The sensor fault signal is defined as

$$f_s(t) = \begin{cases} 0 & \text{if } t \le 5 \\ a_o sin(2\pi f t) & \text{otherwise} \end{cases} \tag{55}$$

where, a_o denotes the magnitude of sensor fault and f shows the frequency. Here we choose $a_o = 0.5$ and $f = 0.5 rad/s$. The selection of amplitude and frequency are based on the operating frequency of the system. In this paper, an outer loop control is achieved using a PID controller design that generates the required pitch and roll tracking path to the multirotor inner loop subsystem. The value of PID gains is obtained from [31].

B. NONLINEAR SIMULATIONS

The simulations are carried out on the 6-DOF UAV system under the influence of external disturbance, sensor fault, and actuator faults. In this regard, three situations are measured to test the presented method performance. Furthermore, to demonstrate the efficiency of the new method, comparative simulations are performed with the existing methods given in [18] and [34].

In the existing FTC method (FTC-I) [18], an adaptive SMC strategy is designed to deal with the actuator faults in

the octorotor UAV system. The adaptive gain is utilized to cope with actuator faults without acquiring the fault information. As a result, it can only manage a limited number of actuator faults and failures. However, the sensor faults can not be addressed by the proposed scheme. In the existing FTC scheme (FTC-II) [34], a sensor and actuator FTC scheme is proposed that first designed an observer to estimate the fault information. Based on the estimated information, an H_∞ observer-based FTC is designed to handle the actuator faults. To compare the performance with the proposed scheme, this scheme is applied to multirotor UAV system.

1) FAULT-FREE CONDITION

In this condition, three distinct commanded reference trajectories are applied to the translational axes states (x, y, and z) where the system is operating under the fault-free situation. The outer loop delivers the anticipated roll, pitch, and yaw commands. The tracking results are provided in Figure 3, which clearly shows the precise reference tracking of the proposed scheme during the nominal condition. However, the results of existing methods [18], [34] are comparable with the proposed method. The control input torques plots are provided in Figure. 4a. The sliding action is still intact, as seen by the switching function in Figure. 4b.

2) ACTUATOR FAULT

In this subsection, the performance of the proposed FTC method is analyzed under faulty conditions, while introducing actuator fault to the nonlinear system. Here, we considered $w_{p_1} = 0.8, w_{p_j} = 0$, and $j = 2, 3, 4$. The plots of the octorotor attitude and translational axes states are presented in Figure 5. In the instance of the suggested technique, the UAV system remained following the planned trajectory despite the loss-of-effectiveness (LOE) of one control input. Whereas, in the case of existing schemes [18], [34], the tracking response has slightly deteriorated from nominal set-point tracking while attaining the desired attitude states. Figure 6a depicts the plot of input torque. Despite LOE the τ_z, and $u_{p_c}(t)$ provided an extra control input according to the estimated fault data. The switching function and estimated value of fault are plotted in Figure 6b. The fault estimation unit passes the estimated information to the control input and the estimation plot is provided in Figure 6b. The ISMC provides strength counter to the disorder and uncertainties in the system that occurred due to nonlinear dynamics and fault estimation error.

$$F_p = \begin{bmatrix} 2.5767 & -4.4457 & -4.5627 & -5.2705 & 1.0274 & -0.3841 & -0.4356 & -0.5637 \\ 1.3314 & -3.1666 & 3.2284 & -2.6352 & 0.5188 & -0.3404 & 0.3665 & -0.2818 \\ 2.3098 & 1.0256 & 0.9139 & -1.0541 & 1.0065 & 0.1382 & 0.0873 & -0.1127 \\ 1.1463 & 0.7016 & -0.6450 & -0.5270 & 0.5022 & 0.0988 & -0.0732 & -0.0564 \\ 2.5767 & -4.4457 & -4.5627 & 5.2705 & 1.0274 & -0.3841 & -0.4356 & 0.5637 \\ 1.3314 & -3.1666 & 3.2284 & 2.6352 & 0.5188 & -0.3404 & 0.3665 & 0.2818 \\ 2.3098 & 1.0256 & 0.9139 & 1.0541 & 1.0065 & 0.1382 & 0.0873 & 0.1127 \\ 1.1463 & 0.7016 & -0.6450 & 0.5270 & 0.5022 & 0.0988 & -0.0732 & 0.0564 \end{bmatrix} \tag{53}$$

$$G_L = \begin{bmatrix} 2.2033 & 0.0000 & 0.0000 & 0.0000 \\ -0.0000 & 2.2033 & 0.0000 & 0.0000 \\ -0.0000 & -0.0000 & 2.2033 & 0.0000 \\ -0.0000 & -0.0000 & -0.0000 & 2.2033 \\ 1.3523 & -0.0000 & -0.0000 & -0.0000 \\ -0.0000 & 1.3523 & -0.0000 & -0.0000 \\ -0.0000 & -0.0000 & 1.3523 & -0.0000 \\ -0.0000 & -0.0000 & -0.0000 & 1.3523 \\ 1.1059 & 0.0000 & 0.0000 & 0.0000 \\ -0.0000 & 1.1059 & 0.0000 & 0.0000 \\ -0.0000 & -0.0000 & 1.1059 & 0.0000 \\ -0.0000 & -0.0000 & -0.0000 & 1.1059 \end{bmatrix}$$

$$F_2 = \begin{bmatrix} -0.4601 & 0.0000 & 0.0000 & 0.0000 \\ 0.0000 & -39.8775 & 0.0000 & 0.0000 \\ 0.0000 & 0.0000 & -39.8775 & 0.0000 \\ 0.0000 & 0.0000 & 0.0000 & -230.0625 \\ 2.1322 & -0.0000 & -0.0000 & -0.0000 \\ -0.0000 & 2.1322 & -0.0000 & -0.0000 \\ -0.0000 & -0.0000 & 2.1322 & -0.0000 \\ -0.0000 & -0.0000 & -0.0000 & 2.1322 \end{bmatrix} \tag{54}$$

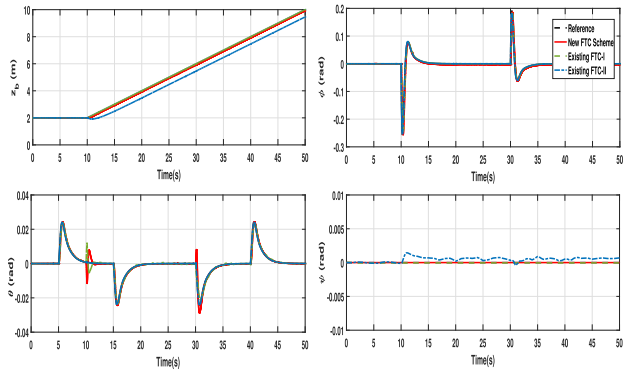

(a)

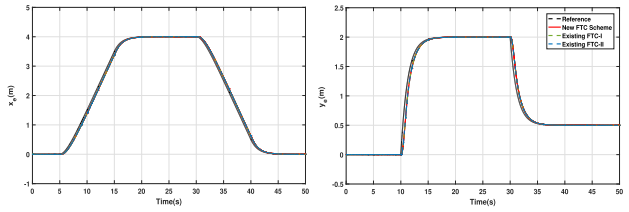

(b)

FIGURE 3. Set point tracking during fault-free condition (a) height, roll, pitch and yaw and (b) x-y position.

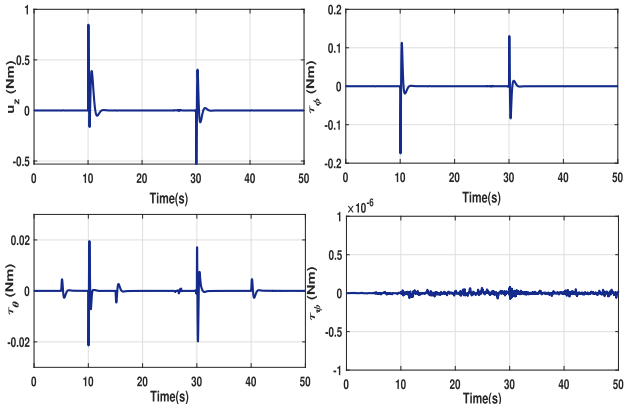

(a)

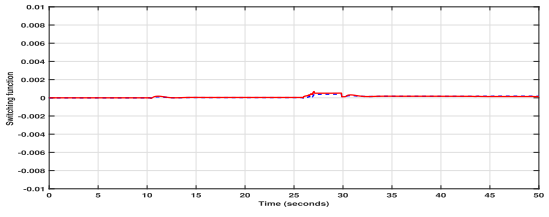

(b)

FIGURE 4. Fault free condition: (a) control inputs plots (b) Sliding mode switching function.

3) SIMULTANEOUS ACTUATOR AND SENSOR FAULT

The actuator and sensor faults are applied to the UAV system, and tracking performance is evaluated under the effect of the proposed FTC method in this scenario, as shown in Figure 7.

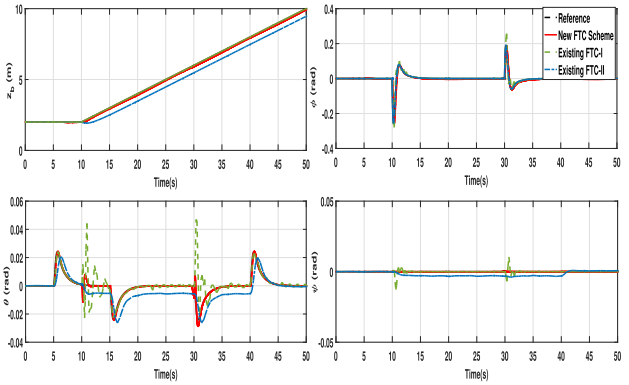

(a)

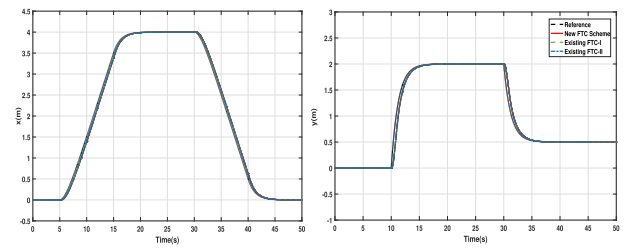

(b)

FIGURE 5. Set point tracking under actuator faults (a) height, roll, pitch and yaw tracking and (b) x-y tracking.

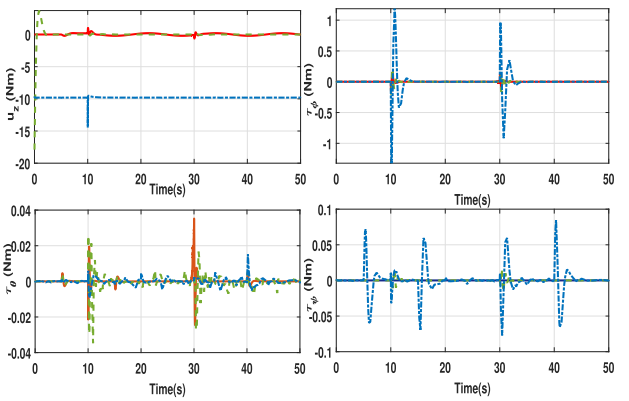

(a)

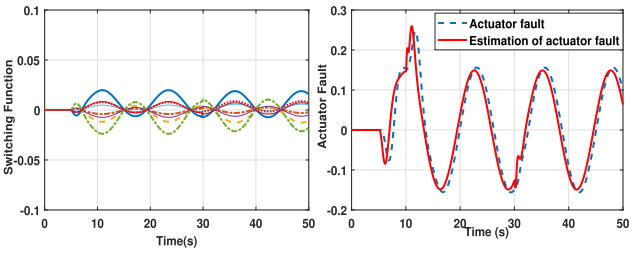

(b)

FIGURE 6. Actuator fault condition (a) control input torques and (b) switching function and actuator fault estimation.

The actuator faults are considered to have 80% LOE of the control input associated with the roll angle rate τ_ϕ and

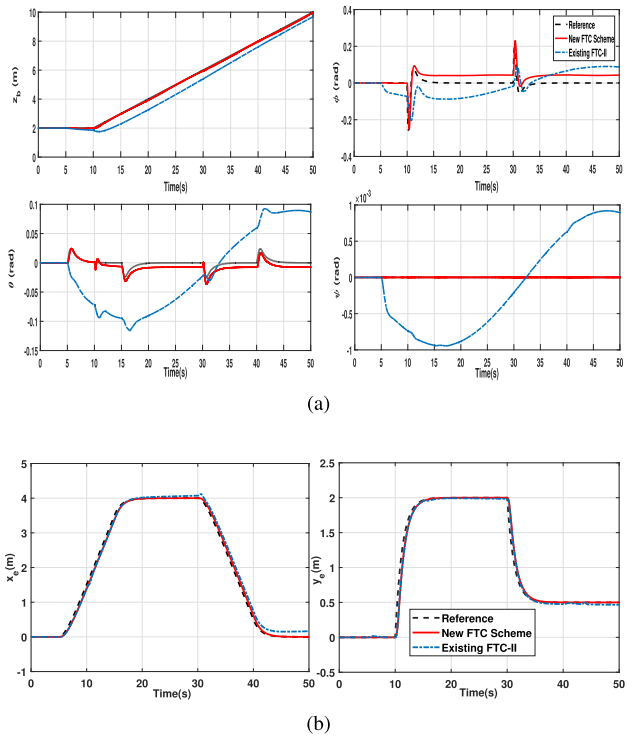

(a)

(b)

FIGURE 7. Set point tracking under actuator and sensor faults (a) height, roll, pitch and yaw tracking and (b) x-y tracking.

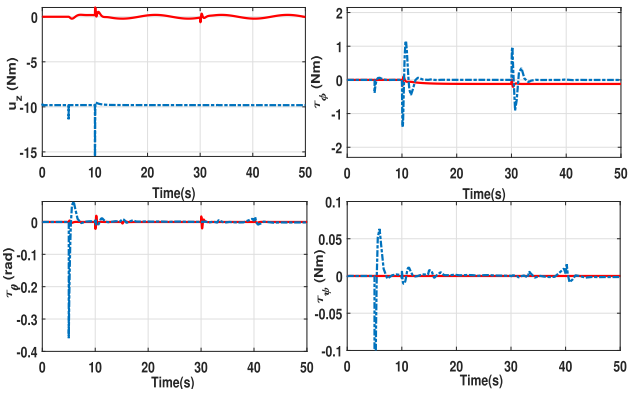

(a)

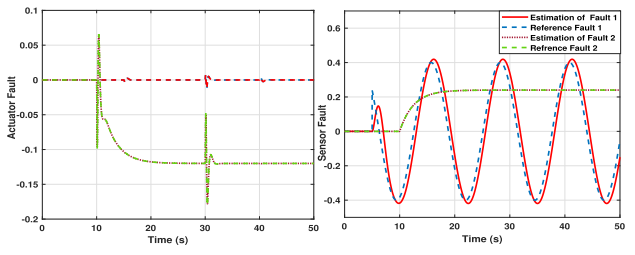

(b)

FIGURE 8. Actuator and sensor fault condition (a) control input torques and (b) sensor and actuator fault estimation.

50% LOE in control input associated with pitch angular rate τ_θ. A sensor fault input signal (55) of amplitude a_o is

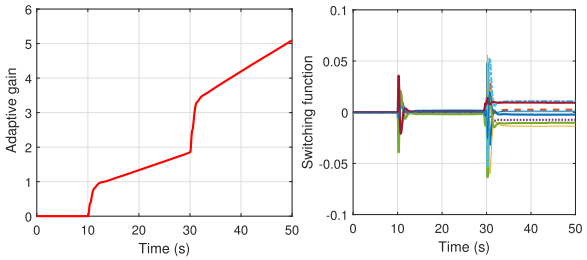

FIGURE 9. Actuator fault condition; adaptive gain and switching function.

applied to the altitude state, and a bias fault signal of amplitude 0.25 is applied to the roll measurement. The tracking performance results are provided in Figure 7. The existing scheme given in [18] is not capable of handling the sensor and actuator faults simultaneously, therefore, the nonlinear simulations are only compared with the existing FTC-II given in [34]. It can be verified that despite the sensor fault and actuator failure, the suggested FTC method is able to follow the desired reference. On the other hand, the existing FTC-II scheme is not precisely following the desired reference input. This demonstrates the effectiveness of the suggested system when compared to other approaches in the literature. In the case of the suggested technique, the coupling of SMC law with the baseline state feedback controller gives better resilience against faults, external disturbances, and model uncertainty than utilizing simply H_∞ based controllers. The fault estimation plot, shown in Figure 8, provides a good estimation of both the actuator and sensor fault input. It can be seen in Figure. 9 that the adaptive law updates the gain to a higher level when the sliding motion jumps out of the sliding manifold. The switching function is plotted in Figure 9 which shows that despite the actuator and sensor fault in the system, the sliding motion is still closer to the setpoint value.

VI. CONCLUSION

In this paper, a fault estimation and fault-tolerant control scheme is proposed for the class of Lipschitz nonlinear uncertain system that is subjected to actuators fault, sensor fault, external disturbance, and uncertainty. An adaptive fault estimation scheme, integrated with H_∞ performance criteria, is first intended to simultaneously estimate the sensor and actuator fault in the nonlinear system. A state feedback-based sliding mode control law is then designed based on the fault data to provide accurate tracking performance in both nominal and faulty conditions. The nonlinear simulations on the full six degrees of freedom model of the multirotor UAV system are performed to validate the efficiency of the projected approach. The performance is evaluated by inducing the fault signal both in the actuator and sensor inputs. Results clearly show that the desired trajectory, even during the faulty condition, remains closer to the nominal system. In future work, the neuroadaptive fuzzy scheme and adaptive fuzzy control scheme [39], [40] will be utilized to achieve tolerance against the uncertain dynamics due to faults and external disturbance. The actuator saturation will also be taken into account in the controller design part.

APPENDIX A

In order to create the bound on the adaptive gain $\rho(t, \hat{x}_p)$, define Lyapunov candidate function as

$$V_3(t) = \frac{1}{2}\delta_p^T(t)\delta_p(t) \tag{56}$$

and the time-derivative, after substituting (39), is obtained as

$$\begin{aligned}\dot{V}_3(t) &= \delta_p^T(t)(-E_p\hat{f}_a(t) - \rho(t,\hat{x}_p)\frac{\delta_p(t)}{\|\delta_p(t)\|} + G_pE_p\hat{f}_a(t)\\ &\quad -G_pM_p\zeta_p(t) + G_pG_{L_p}e_{y_p}(t))\\ &\leq -\|E_p\hat{f}_a(t)\| - \rho(t,\hat{x}_p) + \|G_pE_p\hat{f}_a(t)\|\\ &\quad +\|G_pM_p\zeta_p(t)\| + \|G_pG_{L_p}e_{y_p}(t)\| \end{aligned}\tag{57}$$

Next in order to make the derivative of Lyapunov function negative-definite (i.e. $\dot{V}_3(t) < 0$), we select $\rho(t, \hat{x}_p(t))$ as

$$\begin{aligned}\rho(t,\hat{x}_p(t)) &\geq \|G_pM_p\zeta_p(t)\| + \|G_pE_p\hat{f}_a(t)\|\\ &\quad -\|E_p\hat{f}_a(t)\| + \|G_pG_{L_p}e_{y_p}(t)\| + \eta_s\end{aligned}\tag{58}$$

which satisfies the η_s-reachability condition

$$\delta_p(t)\dot{\delta}_p(t) \leq -\eta_s\|\delta_p(t)\| \tag{59}$$

Hence the finite-time convergence towards the sliding manifold is attained.

The inequality (59) can also be interpreted from the Lyapunov prospective. Define $V_3(t)$ as in (56), then $\dot{V}_3(t) = \delta_p^T(t)\dot{\delta}_p(t)$. From the inequalities in (57-59), it follows

$$\dot{V}_3(t) \leq -\eta_s\|\delta_p(t)\| = -\eta_s\sqrt{2V_3(t)} \tag{60}$$

Integration (60) on both sides we get

$$\sqrt{2V_3(t)} - \sqrt{2V_3(0)} \leq -\eta_s t \tag{61}$$

which implies $V_3(t)$ is less than $\frac{\eta_s}{2V_3(0)}$ unit of time.

ACKNOWLEDGMENT

The authors would like to acknowledge the support of Prince Sultan University for paying the Article Processing Charges (APC) of this publication.

REFERENCES

[1] S. M. Darwish, M. N. El-Dirini, and I. A. Abd El-Moghith, "An adaptive cellular automata scheme for diagnosis of fault tolerance and connectivity preserving in wireless sensor networks," *Alexandria Eng. J.*, vol. 57, no. 4, pp. 4267–4275, Dec. 2018, doi: 10.1016/j.aej.2018.11.012.

[2] E. A. Mahmoud, A. S. Abdel-Khalik, and H. F. Soliman, "An improved fault tolerant for a five-phase induction machine under open gate transistor faults," *Alexandria Eng. J.*, vol. 55, no. 3, pp. 2609–2620, Sep. 2016, doi: 10.1016/j.aej.2016.04.040.

[3] X.-J. Li and G.-H. Yang, "Robust adaptive fault-tolerant control for uncertain linear systems with actuator failures," *IET Control Theory Appl.*, vol. 6, no. 10, pp. 1544–1551, Jul. 2012, doi: 10.1049/iet-cta.2011.0599.

[4] L. Ma, N. Xu, X. Zhao, G. Zong, and X. Huo, "Small-gain technique-based adaptive neural output-feedback fault-tolerant control of switched nonlinear systems with unmodeled dynamics," *IEEE Trans. Syst. Man, Cybern. Syst.*, vol. 51, no. 2, pp. 7051–7062, Nov. 2020, doi: 10.1109/tsmc.2020.2964822.

[5] A. Abbaspour, P. Aboutalebi, K. K. Yen, and A. Sargolzaei, "Neural adaptive observer-based sensor and actuator fault detection in nonlinear systems: Application in UAV," *ISA Trans.*, vol. 67, pp. 317–329, Mar. 2017, doi: 10.1016/j.isatra.2016.11.005.

[6] D. Rotondo, F. Nejjari, and V. Puig, "A virtual actuator and sensor approach for fault tolerant control of LPV systems," *J. Process. Control*, vol. 24, no. 3, pp. 203–222, Mar. 2014, doi: 10.1016/j.jprocont.2013.12.016.

[7] F. Sabbaghian-Bidgoli and M. Farrokhi, "Sensor and actuator fault-tolerant control based on fuzzy unknown input observer: A polynomial fuzzy approach," *Appl. Soft Comput.*, vol. 110, Oct. 2021, Art. no. 107747, doi: 10.1016/j.asoc.2021.107747.

[8] J. Kim, I. Yang, and D. Lee, "Fault tolerant control of wind turbine with sensor and actuator faults," *J. Sens. Sci. Technol.*, vol. 22, no. 1, p. 45, 2013, doi: 10.5369/jsst.2013.22.1.28.

[9] Y. A. Butt, "Robust stabilization of a class of nonholonomic systems using logical switching and integral sliding mode control," *Alexandria Eng. J.*, vol. 57, no. 3, pp. 1591–1596, Sep. 2018, doi: 10.1016/j.aej.2017.05.017.

[10] S. Ijaz, F. Chen, and M. Tariq Hamayun, "A new actuator fault-tolerant control for Lipschitz nonlinear system using adaptive sliding mode control strategy," *Int. J. Robust Nonlinear Control*, vol. 31, no. 6, pp. 2305–2333, Apr. 2021, doi: 10.1002/rnc.5394.

[11] R. T. Y. Thien and Y. Kim, "Decentralized formation flight via PID and integral sliding mode control," *IFAC-Papers Line*, vol. 51, no. 23, pp. 13–15, 2018, doi: 10.1016/j.ifacol.2018.12.003.

[12] V. Sharma, M. Shukla, and B. B. Sharma, "Unknown input observer design for a class of fractional order nonlinear systems," *Chaos, Solitons Fractals*, vol. 115, pp. 96–107, Oct. 2018, doi: 10.1016/j.chaos.2018.08.017.

[13] M. Abbaszadeh and H. J. Marquez, "Robust H_∞ observer design for sampled-data Lipschitz nonlinear systems with exact and Euler approximate models," *Automatica*, vol. 44, no. 3, pp. 799–806, Mar. 2008, doi: 10.1016/j.automatica.2007.07.021.

[14] V. G. Adár, A. M. Stoica, and J. F. Whidborne, "Sliding mode control of a 4Y octorotor," *UPB Sci. Bull. D, Mech. Eng.*, vol. 74, no. 4, pp. 37–52, 2012.

[15] M. Saied, B. Lussier, I. Fantoni, C. Francis, and H. Shraim, "Fault tolerant control for multiple successive failures in an octorotor: Architecture and experiments," in *Proc. IEEE/RSJ Int. Conf. Intell. Robot. Syst. (IROS)*, Sep. 2015, pp. 40–45, doi: 10.1109/IROS.2015.7353112.

[16] S. Zeghlache, H. Mekki, A. Bouguerra, and A. Djerioui, "Actuator fault tolerant control using adaptive RBFNN fuzzy sliding mode controller for coaxial octorotor UAV," *ISA Trans.*, vol. 80, pp. 267–278, Sep. 2018, doi: 10.1016/j.isatra.2018.06.003.

[17] M. Makarov, C. Maniu, and S. Tebbani, "Octorotor UAVs for radar applications: Modeling and analysis for control design," in *Proc. Workshop. Res. Educ. Dev. Unmanned Aer. Syst.*, 2016, pp. 288–297, doi: 10.1109/RED-UAS.2015.7441019.

[18] F. Ejaz, M. T. Hamayun, S. Hussain, S. Ijaz, S. Yang, N. Shehzad, and A. Rashid, "An adaptive sliding mode actuator fault tolerant control scheme for octorotor system," *Int. J. Adv. Robot. Syst.*, vol. 16, no. 2, Mar. 2019, Art. no. 172988141983243, doi: 10.1177/1729881419832435.

[19] M. A. Ashraf, S. Ijaz, Y. Zou, and M. T. Hamayun, "An integral sliding mode fault tolerant control for a class of non-linear Lipschitz systems," *IET Control Theory Appl.*, vol. 15, no. 3, pp. 390–403, Feb. 2021, doi: 10.1049/cth2.12050.

[20] C. P. Tan and C. Edwards, "Sliding mode observers for robust detection and reconstruction of actuator and sensor faults," *Int. J. Robust Nonlinear Control*, vol. 13, no. 5, pp. 443–463, Apr. 2003, doi: 10.1002/rnc.723.

[21] K. Zhang, B. Jiang, and V. Cocquempot, "Adaptive observer-based fast fault estimation," *Int. J. Control. Autom. Syst.*, vol. 6, no. 3, pp. 320–326, 2008.

[22] A. Freddi, S. Longhi, and A. Monteriu, "A model-based fault diagnosis system for a mini-quadrotor," in *Proc. 7th Workshop Adv. Control Diagnosis*, Jan. 2009, pp. 1–20.

[23] Y. Al Younes, H. Noura, A. Rabhi, A. E. Hajjaji, and N. A. Hussien, "Sensor fault detection and isolation in the quadrotor vehicle using nonlinear identity observer approach," in *Proc. Conf. Control Fault-Tolerant Syst.*, Feb. 2013, pp. 486–491, doi: 10.1109/SysTol.2013.6693948.

[24] F. R. Lopez-Estrada, J. C. Ponsart, D. Theilliol, C. M. Astorga-Zaragoza, and Y. M. Zhang, "Robust sensor fault diagnosis and tracking controller for a UAV modelled as LPV system," in *Proc. Int. Conf. Unmanned Aircr. Syst.*, May 2014, pp. 1311–1316, doi: 10.1109/ICUAS.2014.6842389.

[25] H. Rafaralahy, E. Richard, M. Boutayeb, and M. Zasadzinski, "Simultaneous observer based sensor diagnosis and speed estimation of unmanned aerial vehicle," in *Proc. IEEE Conf. Decis. Control*, May 2008, pp. 2938–2943, doi: 10.1109/CDC.2008.4739369.

[26] F. Zhu and Z. Han, "A note on observers for Lipschitz nonlinear systems," *IEEE Trans. Autom. Control*, vol. 47, no. 10, pp. 1751–1754, Oct. 2002, doi: 10.1109/TAC.2002.803552.

[27] C. Aboky, G. Sallet, and J.-C. Vivalda, "Observers for Lipschitz nonlinear systems," *Int. J. Control*, vol. 75, no. 3, pp. 204–212, Jan. 2002, doi: 10.1080/00207170110107256.
[28] G. Lu and D. W. C. Ho, "Full-order and reduced-order observers for Lipschitz descriptor systems: The unified LMI approach," *IEEE Trans. Circuits Syst. II, Exp. Briefs*, vol. 53, no. 7, pp. 563–567, Jul. 2006, doi: 10.1109/TCSII.2006.875332.
[29] S. Ibrir, W. F. Xie, and C.-Y. Su, "Observer-based control of discrete-time Lipschitzian non-linear systems: Application to one-link flexible joint robot," *Int. J. Control*, vol. 78, no. 6, pp. 385–395, Apr. 2005, doi: 10.1080/00207170500101706.
[30] M. J. Khosrowjerdi and S. Barzegary, "Fault tolerant control using virtual actuator for continuous-time Lipschitz nonlinear systems," *Int. J. Robust Nonlin. Control*, vol. 24, no. 16, pp. 2597–2607, Nov. 2014, doi: 10.1002/rnc.3002.
[31] H. Alwi and C. Edwards, "Fault tolerant control of an octorotor using LPV based sliding mode control allocation," in *Proc. Amer. Control Conf.*, Jun. 2013, vol. 9, no. 4, pp. 6505–6510.
[32] S. Bouabdallah and R. Siegwart, "Backstepping and sliding-mode techniques applied to an indoor micro quadrotor," in *Proc. IEEE Int. Conf. Robot. Autom.*, Jan. 2005, pp. 2247–2252, doi: 10.1109/ROBOT.2005.1570447.
[33] A. Victor, "Integral LQR control of a star-shaped octorotor," *INCAS Bull.*, vol. 4, no. 2, pp. 3–18, Jun. 2012, doi: 10.13111/2066-8201.2012.4.2.1.
[34] T. H. Lee, C. P. Lim, S. Nahavandi, and R. G. Roberts, "Observer-based $\mathcal{H}_\infty$ fault-tolerant control for linear systems with sensor and actuator faults," in *IEEE Syst. J.*, vol. 13, no. 2, pp. 1981–1990, Jun. 2019, doi: 10.1109/JSYST.2018.2800710.
[35] H. K. Khalil, *Nonlinear Systems*. Wilmington, DE, USA: Prentice-Hall, 2002.
[36] C. Edwards, H. Alwi, and M. T. Hamayun, "Fault tolerant control using integral sliding modes," in *Proc. Stud. Syst., Decis. Control*, vol. 115, 2018, pp. 305–338.
[37] C. Dai, Y. Liu, and H. Sun, "Fault reconstruction for Lipschitz nonlinear systems using higher terminal sliding mode observer," *J. Shanghai Jiaotong Univ.*, vol. 25, no. 5, pp. 630–638, May 2020, doi: 10.1007/S12204-020-2196-X.
[38] M. Corless and J. Tu, "State and input estimation for a class of uncertain systems," *Automatica*, vol. 34, no. 6, pp. 757–764, 1998, doi: 10.1016/S0005-1098(98)00013-2.
[39] T. Yang, N. Sun, and Y. Fang, "Neuroadaptive control for complicated underactuated systems with simultaneous output and velocity constraints exerted on both actuated and unactuated states," *IEEE Trans. Neural Netw. Learn. Syst.*, early access, Oct. 8, 2021, doi: 10.1109/TNNLS.2021.3115960.
[40] T. Yang and N. Sun. *Adaptive Fuzzy Control for a Class of MIMO Underactuated Systems With Plant Uncertainties and Actuator Deadzones: Design and Experiments*. Accessed: Nov. 29, 2021. [Online]. Available: https://ieeexplore.ieee.org/abstract/document/9345486/

MUHAMMAD AMMAR ASHRAF received the B.Sc. degree in electrical engineering from Bahauddin Zakariya University, Multan, Pakistan, and the master's degree in power electronics and power derives from the Laboratory of Energy Conservation Renewable Energies, Beijing University of Aeronautics and Astronautics, Beijing, China, in 2016. He is currently a doctoral candidate with the University of Science and Technology, Beijing. His main research interests include modeling and fault-tolerant control of aircraft systems, sliding mode control, and robust control.

SALMAN IJAZ received the Ph.D. degree in control sciences and control engineering from Beihang University (BUAA), Beijing, in 2018. He then joined the Nanjing University of Aeronautics and Astronautics (NUAA) to pursue his postdoctoral studies where he worked for two years. He is currently serving as an Assistant Professor for the School of Aerospace, University of Nottingham, Ningbo, China. His research interests include the modeling and fault-tolerant control of aircraft systems, sliding mode control, control allocations, robust control, and unmanned aerial vehicles.

UMAIR JAVAID received the Ph.D. degree in control sciences and control engineering from Beihang University (BUAA), Beijing, in 2019. He is currently pursuing the postdoctoral degree with the Nanjing University of Aeronautics and Astronautics, Nanjing, China. His research interests include the modeling and fault-tolerant control of spacecraft systems, robust control, and sliding mode control.

SHARIQ HUSSAIN received the master's degree in computer science from PMAS Arid Agriculture University, Rawalpindi, Pakistan, in 2007, and the Ph.D. degree in applied computer technology from the University of Science and Technology Beijing, Beijing, China, in 2014. He is an Associate Professor at the Department of Software Engineering, Foundation University Islamabad, Pakistan. His main research interests include web services, QoS in web services, web service testing, the IoT, context awareness, and e-learning. He served as a Workshop/Special Session Co-Chair for IEEE International Conference on Internet of People 2018 (IoP 2018) and the Publicity Chair for IEEE International Conference on Internet of People (IoP 2015). He is also serving as a Guest Editor for *SN Applied Sciences* (Special Collection: IoT in Mobile, Big Data Analytics and Cloud Computing) and an Editorial Board Member of *Journal of Next Generation Information Technology* (JNIT)—AICIT, Republic of Korea.

HARIS ANWAAR received the Ph.D. degree in control science and engineering from the University of Science and Technology, Beijing, in 2018. He is an Assistant Professor at the Electrical Department of University of Engineering and Technology (UET) Lahore (New Campus). His main research interests include iterative learning control, fractional order control, and fault tolerant control.

MOHAMED MAREY received the M.Sc. degree in electrical engineering from Menoufia University, Egypt, in 1999, and the Ph.D. degree in electrical engineering from Ghent University, Belgium, in 2008. From 2009 to 2014, he was a Research Associate and a Visiting Professor with the Faculty of Engineering and Applied Science, Memorial University, Canada. He is currently working as the Research Laboratory Leader of the Smart Systems Engineering Laboratory, College of Engineering, Prince Sultan University Riyadh. He has authored the book *Multi-Carrier Receivers in the Presence of Interference: Overlay Systems* (VDM Publishing House Ltd., 2009) and around 100 scientific papers published in international journals and conferences. His main research interests include wireless communications and digital signal processing, with a particular focus on smart antennas, cooperative communications, signal classification for cognitive radio systems, synchronization and channel estimation, multiple-input multiple-output antenna systems, multicarrier systems, and error correcting codes. He was a recipient of the Young Scientist Award from the International Union of Radio Science, in 1999. He serves as an Editor for the IEEE Open Journal of the Communications Society.